Ontogeny of Swimming Movements in the Catfish *Clarias gariepinus*

Quentin Mauguit[1,*], Vincent Gennotte[2], Christophe Becco[3], Etienne Baras[4], Nicolas Vandewalle[3] and Pierre Vandewalle[1]

[1]*Functional and Evolutive Morphology Laboratory, University of Liège, Belgium;* [2]*CEFRA, University of Liège, Belgium;* [3]*GRASP, University of Liège, Belgium;* [4]*IRD-GAMET Montpellier, France*

Abstract: The swimming movements of *C. gariepinus* larvae were recorded with a high-speed camera (400, 500 and 800 fps) from 0 to 336 hours post-hatching. Movements of adult fish were also recorded to provide information on the last developmental stage. Seven landmarks positioned on the fish midline were used during tail beating to determine various parameters during ontogeny and, on the basis of these parameters, to describe the first appearance of swimming movements and their development and efficiency during growth.

Larvae were unable to swim at hatching (4 mm total length). Swimming movements were established at 48 hours post-hatching when the fish measured between 7 and 8 mm total length and the yolk sac was more than 95% absorbed. At this stage, lateral excursion of the head appeared strongly reduced (from 13% to 6% of the total length). The efficiency of swimming movements increased throughout ontogeny, as did the homogeneity of the speed of the propulsive wave. Spontaneous swimming speed of 1 to 10 TLs^{-1} were observed in early stage (8-12 hPH). The various speed induced significant variations in parameters such as the amplitude of lateral head movements, swimming efficiency, and body rigidity. No major change was observed at the theoretical flow-regime transition.

Keywords: Larvae, swimming, ontogeny, catfishes, strouhal number.

INTRODUCTION

All fish larvae and most adult fish move by executing undulatory movements with their bodies. Swimming movement corresponds to the propagation of a wave of increasing amplitude from head to tail [1]. This wave results from the combined effects of mechanical properties of the body, muscle activity, and interactions between the fish body and the surrounding water [2-4]. The three main undulatory swimming modes are anguilliform, subcarangiform and carangiform mode. Previous studies dealing with the ontogeny of routine swimming movements in fish have only concerned the carangiform and subcarangiform modes of swimming (carangiform: the cyprinid *Danio rerio* (Hamilton) [5-8], the cyprinid *Cyprinus carpio* L. [9-11], the pleuronectid *Pleuronectes Platessa* L. [12,13]; subcarangiform: the clupeid *Clupea harengus* L. [14]). To our knowledge, no rigorous study has addressed the ontogeny of anguilliform mode of swimming.

The undulatory swimming mode enables fish to better exploit the resistance forces of the medium [15]. It is efficient in all types of hydrodynamic flow regime that an organism may encounter while moving in a liquid medium [3, 16]. The flow regime depends on the total length (TL) of the animal, its swimming speed (U), and the kinematic viscosity of the fluid (v). The ratio of the viscous and inertial forces of the fluid can be determined by calculating the Reynolds number (Re): $Re = UTLv^{-1}$ [17]. At hatching, larvae measure only a few millimeters and they move in an intermediate flow regime, corresponding to $50 < Re < 900$ [7]. They must deal with the viscosity and inertial forces of the medium [18-19]. Adult fish, on the other hand, move only in an inertial flow regime, corresponding to $Re > 1000$ [17], because the viscous forces can be considered negligible. During growth, larvae thus experience a hydrodynamic regime change [19] that might affect the execution of swimming movements during ontogeny. Additional morphological changes can have some effects on swimming movements: yolk-sac absorption [5, 20], neural system development [21], transformation of the notochord into a vertebral column [21-23], replacement of the finfold by fins sustained by skeletal elements [24,25], changes in the type of muscle fiber, and changes in axial muscle system morphology [26].

During the execution of an undulatory movement and in an earth frame of reference, each body segment follows an undulating path that looks like a pure sine if the swimming speed is constant and the amplitude is small [3]. These conditions are violated to a greater or lesser extent in real fish, where the body wave amplitude increases from head to tail, with a minimum amplitude near the head-body transition [27]. Consequently, the propulsive waves deviate least from a sine near this pivot point and more strongly at the tail, where the lateral movement amplitude is maximal. Moreover, fish swimming speed is not constant during a tail beat. Undulatory thrust oscillates as the tail beats back and forth, and so does the swimming speed [5]. These oscillations are small in the inertial flow regime; but swimming speed oscillates substantially in fish larvae swimming in the viscous and intermediate flow regimes [5]. The oscillations also decrease with yolk-sac absorption.

*Address correspondence to this author at the Functional and Evolutive Morphology Laboratory, University of Liège, Allée de la Chimie 3 Bât B6c, 4000 Liège, Belgium; Tel: +3243665033; E-mail: q.mauguit@ulg.ac.be
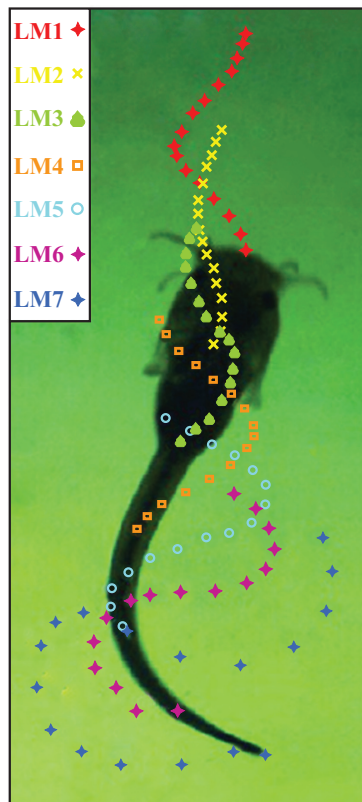
Fig. (1). *Clarias gariepinus* larva measuring 10 mm TL. Each of the seven colored paths represents the trajectory of one of the seven equidistant landmarks (LM1, LM2...) during execution of one complete undulatory swimming movement.

The present study focuses on the development of regular swimming movements in the silurids *Clarias gariepinus* (Burchell). The ontogeny of swimming movements in post-hatching larvae is described, mathematically characterized and compared to the anguilliform movements of adult fish. We expected the propulsive wave to deviate from a pure sine in all age groups, but to deviate less and less with increasing body length and swimming speed. Our hypothesis is mainly based on the fact that swimming speed of an oscillating propeller oscillates more strongly in the viscous flow regime of slow, small swimmers than in the inertial flow regime of long, fast swimmers [5]. We also examined the relationship between swimming movements and two major ontogenic events: yolk-sac absorption and the theoretical hydrodynamic flow-regime change.

MATERIALS AND METHODOLOGY

Clarias gariepinus larvae were obtained by reproducing genitors raised at the Tihange Aquaculture Research Station (CEFRA, University of Liege, Tihange, Belgium). The average temperature during the experiment was 28.0±0.2°C and the photoperiod was a 12 D : 12 L light:dark cycle. A temperature included in the range of 25-28°C corresponds to the situation where the energy and proteins (provided among other thing by the yolk-sac) are most efficiently used for the *C. gariepinus* growth [28]. This species has both night and day feeding activities but shown a preference for diurnal feeding in the 12D : 12 L photoperiod [29]. Consequently, from 48 hours post-hatching (hPH), the larvae were fed on

Artemia salina nauplii 4 to 5 times a day, exclusively during daylight hours. They were haphazardly sampled at 0, 4, 8, 12, 16, 20, 24, 30, 36, 42, 48, 60, 72, 96, 120, 144, 168, 192, 216, 264, and 312 hPH. Adult swimming movements of 5 fish (TL 129 to 156 mm) were also recorded.

Batches of larvae were recorded at frame rates of 400, 500, or 800 fps (exposure time 245, 200, and 125 μs, respectively) with a high-speed digital camera (RedLake Motion-Pro 2000, San Diego, CA, USA). The frame rate depended on the time that took the fish to execute a complete swimming movement. The video recording of small larvae (from 0 to 168hPH) was realized in a 75 x 25 mm aquarium, and the camera was mounted on a dissection microscope (Olympus SZ40). Movements of fish exceeding 10 mm (from 192 to 336hPH), were recorded in a 150 x 75 mm aquarium by using a lens attached directly to the camera (Linos Mevis 25 mm, 1.6:16) and a 5-mm extension ring. The height of the water was limited from 7 to 15 mm for larvae according to the size of the fish and in order to avoid the formation of surface waves during fish swimming movements (the depth was at least 5 times the height of the fish body). The field was lit from the top and bottom with two Volpi 6000-1 cold light sources and four optical fibers. Adult fish were monitored in a 1500 x 250 mm tank and the field was lit with two halogen lamps (IFF, Q-1250). A 25-mm lens was used without an extension ring. The height of the water was limited to 50 mm. For each developmental stage, video sequences of fish swimming in a straight line and performing at least one complete tail beat cycle were recorded. Only continuous swimming movements executed after the acceleration phase associated with the initiation of the movements were recorded. Fish were free to move in all directions and at variable swimming speeds.

Although video sequences were recorded from hatching onwards (4.0 ± 0.1mm TL), it was impossible to analyze the movies recorded before 8 hPH (5.3 ± 0.4mm TL). Larvae made many non-swimming movements, and during a video sequence they rotate around yolk sac.

Analyses were carried out with Midas software (RedLake, version 2.1.1). Ninety-three sequences were analyzed in an earth-bound frame of reference. The fish midline was divided into 6 equal segments, and 7 landmarks were determined between the snout and the tail tip, *i.e.* at 0, 0.14, 0.29, 0.43, 0.57, 0.71, 0.86 and 1 TL (respectively LM1 to LM7, Fig. **1**). During the analyses, the x axis was defined as the axis of the direction of fish displacement. The amplitudes of the movements of the various landmarks were plotted on the y axis (perpendicular to the x axis). The (x; y) coordinates of each landmark were mathematically transformed so as to move the first point of each landmark's trajectory to the origin of an orthogonal referential and to make the x axis coincide with the displacement axis of the fish. Besides studying in detail the motion followed by the landmarks, this method allows to compare these movements between different landmarks or fish.

At each ontogenetic stage, fish and their movements were characterized by a series of direct and indirect parameters: total fish length (TL, mm), yolk-sac volume (Vv, cm³), oscillatory movement period (T, s), relative swimming speed (U, TLs^{-1}), the amplitude of each landmark (A$_{1-7}$, proportion of

TL), and the Reynolds number (Re). Yolk-sac areas in the frontal plane (S) were determined with Vistametrix software (Skillcrest, version 1.34). Yolk-sac volumes were calculated as follows, assuming a spheroid shape: $V_v = (4/3)\pi * (S\pi^{-1})^{1.5}$.

Preliminary analyses were conducted to test the number of frames to be analyzed. All the parameters were calculated on the basis of all the frames for one sequence at three developmental stages (12 hPH, 120 hPH and 336 hPH). The same parameters were then calculated by analyzing one frame out of two, three, four and five. The results obtained were compared to the first ones (full sequences). Accepting no more than a 5% difference between the results obtained for the full and subsampled sequences, it proved sufficient to record the landmark positions on frames 5 or 6 ms apart (11 to 19 frames were analyzed per video sequence).

A new index was defined to study the establishment of the swimming movements. It is based on the comparison of the observed movements followed by the landmarks with theoretical trajectories defined mathematically for each of them. Fish swimming movements can be described as undulatory phenomena characterized by a wavelength and an amplitude [3]. From a distribution of the observed values of x, and knowing the movement amplitude (A_{1-7}) and its wavelength, a theoretical sinusoid could be calculated for the various landmarks at each stage of development. The sinusoidal function linking y_{th} (theoretical y) and x is $y_{th} = A \sin(\omega x + \varphi)$, where A is the amplitude (in mm), ω the pulsation (in radians mm^{-1}), and φ the initial phase (in radians). A and ω were determined from the observed coordinates: $A = y_{max}$ and $\omega = 2\pi T_x^{-1}$, where y_{max} is the maximum amplitude observed during one tail beat and T_x is the period of the motion. Calculation of φ was done to obtain the best fit between the observed and theoretical curves. For each landmark, the y_{th} values were calculated by varying φ between 0 and 2π by increments of 0.01 radian (this yields 628 theoretical sinusoids). The φ value of the theoretical sinusoid having the best fit (the highest r²) with the observed motion was then selected. These sinusoids correspond to the theoretical ideal trajectories each landmark should follow during execution of a complete undulatory movement. The paths observed for the various larval landmarks throughout ontogeny were compared to these theoretical sinusoids. Larval motion was compared with adult motion because the adult represents the final development stage. The coefficient of determination (r^2_{1-7}) of the relationship between the experimental motion of a landmark and its associated sinusoid provided an objective index of the similarity between this motion and the adult sinusoid motion. The mean of the r^2_1 to r^2_6 values of a fish specimen (r^2_{mean}) yielded a global index of the establishment of movements at a specific developmental stage. The r^2_7 value was not used in the calculation of this index, because the seventh landmark was situated at the tip of the caudal fin and not on the body. The caudal fin is a relatively soft structure, and fish larvae are unable to control fully their tail-tip movements. Muscle control of fin rays exists, but actinotrichia might not exert the same kind of control because of their simpler internal structure and/or lack of control muscle. The coefficient of variation of r² for the different landmarks (CV r²) was used to gauge whether, at a

given developmental stage, the movement appeared to have reached the same level of organization in different parts of the body. According to the results, the movements of each landmark were analyzed as a function of body length.

It was possible to determine the propagation speed of the wave along the body between two successive landmarks during execution of a swimming movement. Calculation of the coefficient of variation of $\Delta\varphi$ (CV $\Delta\varphi$) enabled to characterize the steadiness of the wave through the body of the fish. $\Delta\varphi$ represents the disparity of phase differences measured between each two consecutive landmarks placed on the midline of the fish. Values of the coefficient close to 0 mean that the wave traverses the fish's body at a constant speed.

The Strouhal number (*St*) is a dimensionless number used to describe the kinematics of the tail or wings of an animal as it swims or flies [30]. It is calculated according to the formula: $St = fA_7U^{-1}$, where f is the tail-beat frequency ($f = T^{-1}$, Hz), A_7 represents the maximum amplitude of the tail movement (unit: TL), and U is the relative swimming speed (in TLs^{-1}). In biology, the Strouhal number can be regarded as a propulsion efficiency index. Propulsive efficiency, defined as the ratio of hydrodynamic power output to mechanical power input [31], is optimal for adults (inertial flow regime) when the Strouhal number ranges from 0.2 to 0.4 [32,33].

The movements of the anterior part of the body contribute to increasing the drag of the fish and thereby reduce its swimming efficiency [34]. Consequently, special attention was paid to the variation of head-movement amplitude throughout ontogeny and in relation to the swimming speed. Great attention was also paid to the amplitude movements (and not on the trajectory) of the tip of the caudal fin.

To establish which of two factors, age post-hatching or total fish body length, correlates more strongly with development progress, several multiple polynomial regressions of the third degree were performed. Analyses were applied to the studied parameters (dependent variable: Z; see the following regression model) on the one hand and the age post-hatching and total fish length (independent variables, X and Y) on the other. The regression model could be written as $Z = \beta_0 + \beta_1*X + \beta_2*X^2 + \beta_3*X^3 + \beta_4*Y + \beta_5*Y^2 + \beta_6*Y^3$, where β_0 is the intercept and β_{1-6} are the partial regression coefficients. X and Y are determinants; they were included in the model only if they were significant (established through the use of a T-test). The best-fit model was identified in a stepwise forward-selection manner by running Statistica (Statsoft, version 8.1) and was selected on the basis of the lowest p-value.

In the study of parameter changes according to the best reference for ontogeny (age or total fish length), the effects of swimming speed were also investigated by means of several multiple polynomial regressions of the third degree. In the event of a significant effect of swimming speed on the fluctuations of a parameter, the data were presented in surface plots. The surface was fitted to the best of the points of observation by the weighted least squared distance method.

Coefficients of correlation were calculated in order to characterize the relationship between yolk-sac absorption and some of the other studied parameters. Mann-Whitney U tests were performed to compare the index values obtained
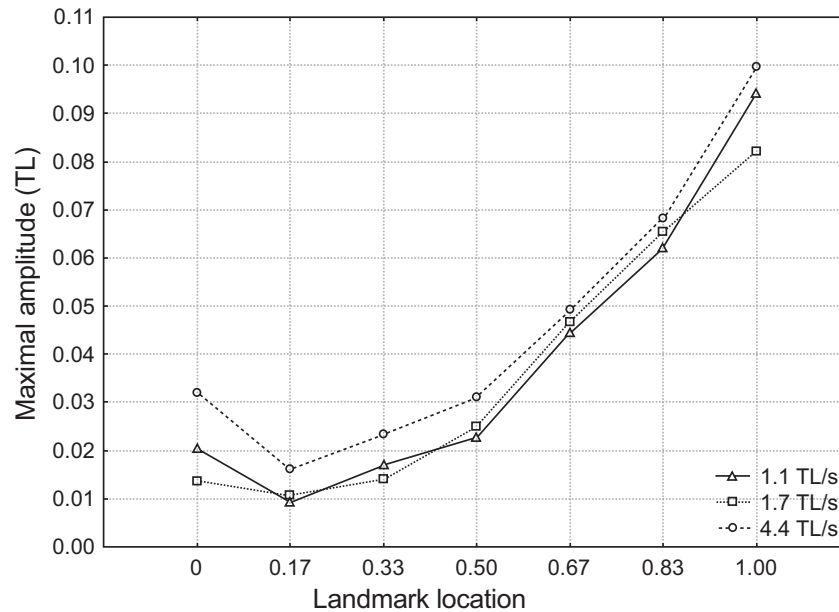
Fig. (2). Maximum amplitudes of the various landmarks (LM1=0% and LM7=100% of the total fish length) placed on adult *Clarias garie-pinus* specimens. Results are given at three different speeds: 1.1 TLs^{-1} (triangle), 1.7 TLs^{-1} (square), and 4.4 TLs^{-1} (circle).

for the five biggest larvae with the index value determined for the adults.

RESULTS

Final Developmental Stage

As supposed by looking at some morphological traits (as the elongated body and well-developed anal, dorsal, and caudal fins), the swimming mode of adult *Clarias gariepinus* can be considered as anguilliform. The maximum amplitude of lateral excursions was recorded as a function of the position along the body from head (left) to tail (right; Fig. **2**). The whole body appeared to undulate from a pivot point located far ahead on the body (at 0.17 %TL). Moreover, more than one wavelength was observed on the fish body.

The swimming speed affects the movements of various body parts (Table **1**). Indeed, the amplitude of the head movements had been found to depend on the swimming speed (Table **1**, Fig. **2**). Moreover, between 1 and 2 TLs^{-1}, the amplitude of the movements (LM 3 to 6) decreased with increasing swimming speed. In this speed range, the values ranged between 1 and 2 %TL. From 2.5 TLs^{-1}, the amplitude increased. At 4.4 TLs^{-1}, the amplitude of the head movements represented 3% of the total fish length. No correlation was found between tail-movement amplitude and swimming speed ($F_{2,2}$=0.935, P=0.517). Whatever the swimming speed, the caudal fin was found to move with an amplitude ranging from 8 to 13% of the total fish length.

At the adult stage, swimming movements were well established, since they follow sinusoidal path (r^2_{mean}>0.95), and seems to be better executed when the swimming speed increases. However, multiple regression showed that this relationship was not significant (P=0.051; Table **1**). It appears that the value of the coefficient decreased between 1 and 2.5 TLs^{-1} but increased at speeds superior to 2.5 TLs^{-1}. Table

1 shows that the index varied like the square of the swimming speed, since swimming speed appears as a determinant in the regression model.

Variations of the propulsive wave speed along the adult fish body were not consistent. The mean value of CV $\Delta\varphi$ at the adult stage was 7.69±6.03%. Swimming speed was not found to correlate with the CV $\Delta\varphi$ coefficient ($F_{1,3}$=0.946, P=0.402).

Swimming efficiency increased with swimming speed (Table **1**). Between 1 and 2 TLs^{-1}, the Strouhal value observed were greater than 0.4 but inferior to 0.8. At 4.5 TLs^{-1}, an optimally efficient swimming movement was observed ($St = 0.32$).

Ontogeny of Swimming Movements

Larvae measured approximately 4 mm at hatching. Their size increased rapidly up to 144 hPH (TL: 10.24 ± 0.11 mm), then their growth slowed down. Their maximum size, reached after 312 hPH, was 20.5 mm. The mean volume of the yolk sac was 1.35 ± 0.07 mm³ at hatching. Its absorption was complete by 60 hPH (TL: 8.54 ± 0.10 mm).

The total fish length has been used as the reference for studying ontogenetic events. Multiple polynomial regressions showed a more significant correlation of all coefficients with total fish length. For each index, the total length is the only determinant (or total length squared) in the regression equations (Table **2**).

The total fish length clearly influences the motion of seven landmarks placed on the medio-dorsal line. This is shown for two representative fish measuring 5.5 and 10 mm respectively in Fig. (**3**) (left vs. right column). At the 10-mm stage, the trajectories of the landmarks (except for LM7 at the tail tip) matched quite closely the theoretically determined sinusoids. At this size, *C. gariepinus* displays estab-

Table 1. Results of the Multiple Polynomial Regressions Done in Order to Characterize the Effects of the Relative Swimming Speed on the Evolution of the r^2_{mean} and *St* Indexes and on the Amplitude Head-Tip (LM1) Movement in *Clarias gariepinus*.

Determinant	Partial Regression Coefficient	Standard Error on Estimate	0.95 Confidence Interval	Significance of the Variables (T-test)	
r^2_{mean} ($F_{2,2}$=18.625, P=0.051)					
Intercept: 1.1015					
Swimming speed (L_T/s)	-0.0464	0.0103	-0.0262 to -0.0666	t_2=-4.51	P=0.046
[Swimming speed (TL/s)]²	0.0089	0.0018	-0.0054 to -0.0124	t_2=4.87	P=0.040
St ($F_{2,2}$=498.53, P<0.002)					
Intercept: 0.5790					
Swimming speed (TL/s)	-0.2921	0.0166	-0.2596 to -0.3246	t_2=-17.55	P=0.003
[Swimming speed (TL/s)]²	0.0446	0.0030	0.0504 to 0.0387	t_2=15.02	P=0.004
Amplitude LM1 ($F_{2,2}$=395.19, P=0.002)					
Intercept: 0.0441					
Swimming speed (TL/s)	-0.0274	0.0018	-0.0239 to -0.0309	t_2=-15.34	P=0.004
[Swimming speed (TL/s)]²	0.0056	0.0003	-0.0050 to 0.0062	t_2=17.48	P=0.003

Total variance explained for r^2_{mean}, 94.6%; for *St*, 99.8%; for Ampl. LM1, 99.7%.

Table 2. Results of the Multiple Polynomial Regressions Performed in Order to Characterize the Effects of Age or Size on the variation of the r^2_{mean}, CV r², CV Δφ, and *St* Indexes for *Clarias gariepinus* Larvae

Determinant	Partial Regression Coefficient	Standard Error of Estimate	0.95 Confidence Interval		Significativity of the Variables (T-test)	
r^2_{mean} ($F_{2,73}$=59.316, P<0.0001)						
Intercept: -6.2545						
Total length (mm)	19.346	0.3679	12.135	to 26.557	t_{73}=5.2579	P<0.0001
[Total length (mm)]²	-0.0945	0.0223	-0.1382	to -0.0508	t_{73}=-4.2292	P<0.0001
CV r² ($F_{2,73}$=56.737, P<0.0001)						
Intercept: -1.3621						
Total length (mm)	-0.2686	0.0464	-0.3595	to -0.1777	t_{73}=-5.7764	P<0.0001
[Total length (mm)]²	0.0136	0.0028	0.0081	to 0.0191	t_{73}=4.8065	P<0.0001
CV Δφ ($F_{2,73}$=9.2515, P=0.0033)						
Intercept: 0.8615						
Total length (mm)	-0.0427	0.0141	-0.0703	to -0.0151	t_{73}=-3.0416	P=0.0033
St ($F_{2,73}$=9.8162, P=0.0025)						
Intercept: 0.8689						
[Total length (mm)]²	-0.0019	0.0006	-0.0031	to -0.0007	t_{73}=-3.0416	P=0.0025

Total variance explained for r^2_{mean}, 61.9%; for CV r², 60.8%; for CV Δφ, 11.1%; for *St*, 11.7%.
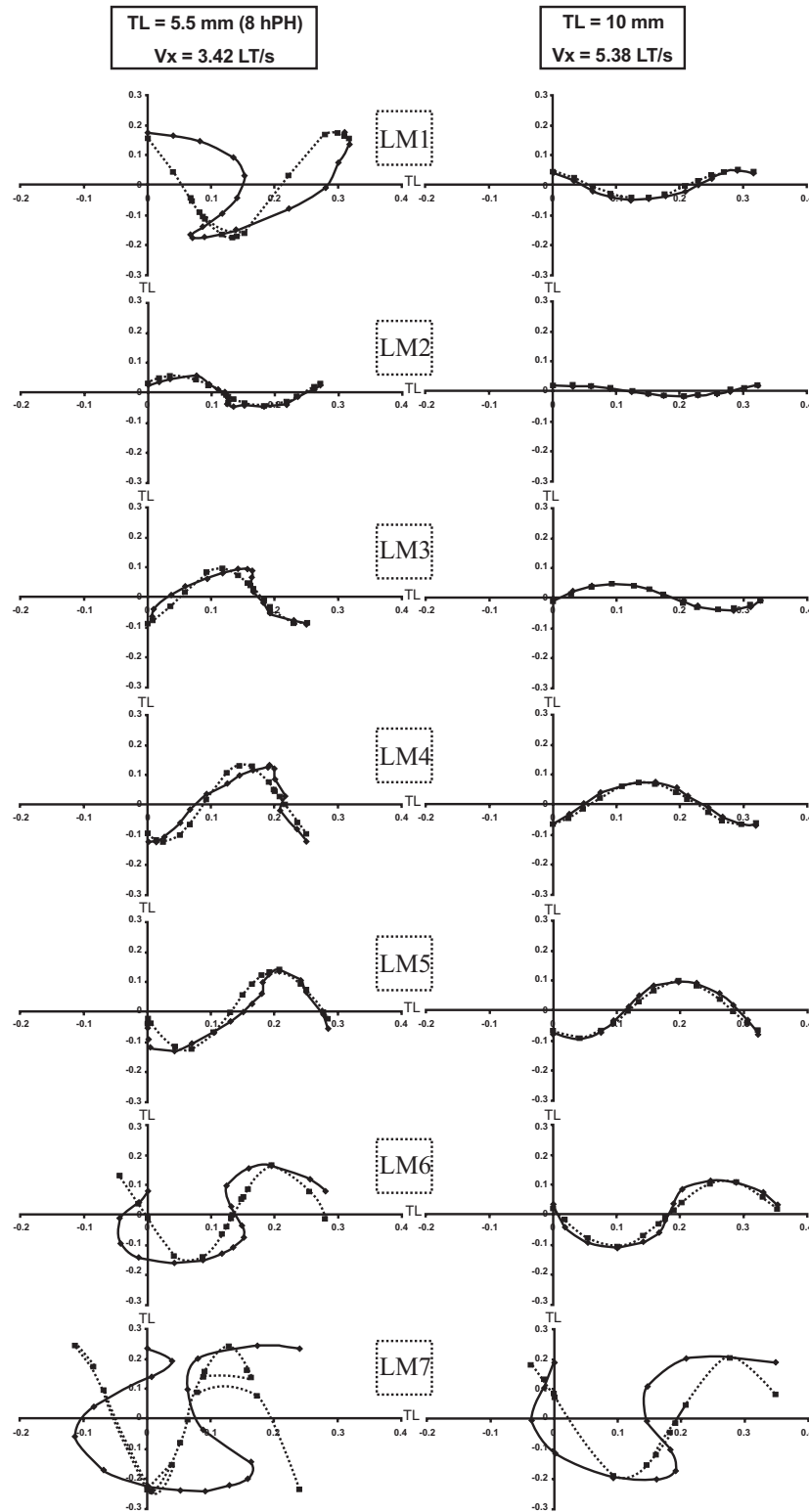
Fig. (3). Trajectories of the seven landmarks on two *Clarias gariepinus* larvae, one measuring 5.5 mm TL and the other, 10 mm TL (left and right column, respectively) during execution of one complete undulatory swimming movement. LM1 is located at the head-tip and LM7 at the tail-tip. Each continuous line shows the observed trajectory and dotted line represents the theoretical sinusoid calculated from the observed path (and which should correspond to adult motion). The data on the x and y axes are expressed as percentages of the total length of the observed fish. For LM6 and LM7 on the 5.5-mm fish and for LM7 on the 10-mm fish, the landmark trajectories do not approach a sinusoid form. Therefore, it was impossible to determine the theoretical trajectory that should be followed by the landmark.
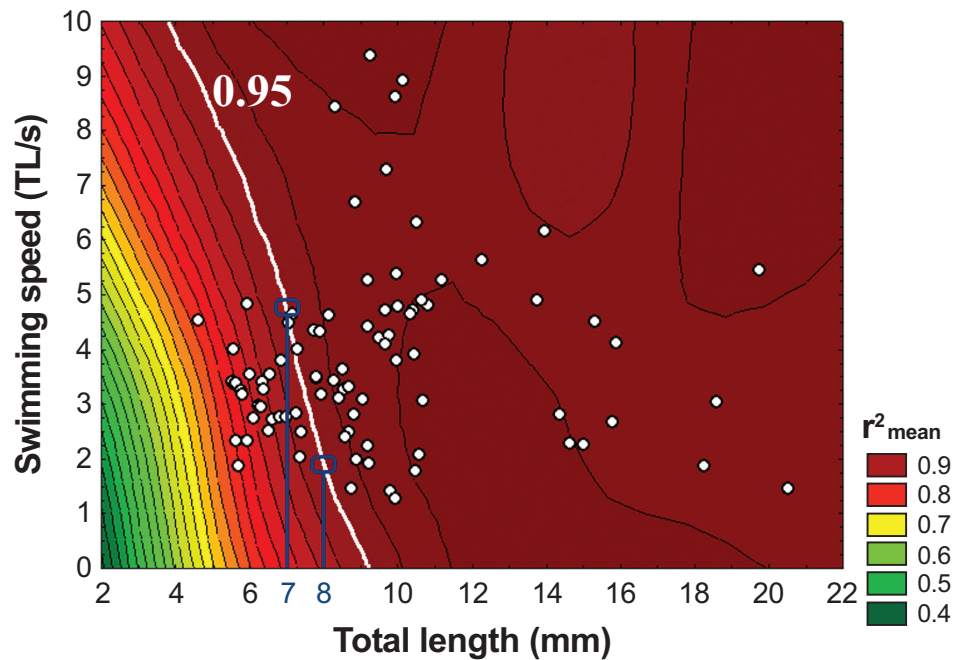
Fig. (4). Surface plot representing the variation of r^2_{mean} as a function of the total length and relative swimming speed of *Clarias gariepinus* larvae. The index value increases when, while moving on the plot, the color of the area changes from dark green to dark red. White circles: observations made during the present study; each point representing a fish. White line: threshold value of 0.95. To the right of this line, swimming movements are established. Blue lines give information on the relative swimming speed that a fish must attain in order to practice adult swimming movements, according to the total length.

lished adult-like swimming movements. On the other hand, the trajectories of the landmarks placed on the 5.5 mm TL fish, especially LM1, LM6, and LM7, did not coincide with the adult sinusoidal path. Moreover, the movements of all landmarks showed a reduced amplitude at the 10 mm stage as compared to the 5.5 mm one, this reduction being greater for LM1. Whatever the size, the movements of least amplitude were observed just behind the head (LM2). The position of this pivot point did not seem to move significantly along the body of the animal during growth. For the longest larvae studied, the average maximum amplitudes of the landmark movements, expressed as percentages of total fish length, were as follows (swimming speed is not taken into account): $5.1 \pm 0.7\%$ for LM1, $2.1 \pm 0.5\%$ for LM2, $3.5 \pm 0.4\%$ for LM3, $5.9 \pm 0.1\%$ for LM4, $7.9 \pm 1.4\%$ for LM5, $11.8 \pm 1.4\%$ for LM6, and $21.2 \pm 1.4\%$ for LM7. These last results could be use to justify, among other things, the adult anguilliform swimming mode.

Swimming movements were not established when the first of them were observed since the path followed by the landmarks differed from sinusoids. During growth, the r^2_{mean} index was shown to increase up to the plateau value of 0.95 characteristic of adult swimming behavior (Fig. **4**). The plot shows that the position of this plateau varied according to the size and swimming speed. Indeed, total fish length and swimming speed both appeared significantly in the polynomial regression equation (Table **3**). The swimming speed of the smallest fish varied between 2 and 5 TLs^{-1}. In this speed range, the larvae were able to swim like adult fish when they have a total length between 7 and 8 mm TL. At 7 mm TL, the fish had to swim faster (4.8 TLs^{-1}) in order to execute correct swimming movements completely, whereas fish

measuring 8 mm TL could execute their swimming movements perfectly at only 2 TLs^{-1} (Fig. **4**). Nine millimeters emerges as the length at which all fish could perform adult-like swimming movements independently of the relative swimming speed.

Physical consideration could not explain these observations while the yolk sac absorption could. All landmark trajectories became well established while the fish were still moving in a non-inertial hydrodynamic flow regime (Re<1000; Fig. **5A**). Improvement of the trajectory of each landmark was significantly correlated to the absorption of the yolk sac (R = -0.65, P<0.001). As a very strong correlation was also evidenced between total fish length and yolk-sac absorption (R = -0.69, P<0.001), it was not surprising also to observe a strong correlation between total fish length and the establishment of swimming movements (R = 0.51, P<0.001). In the future, it will be necessary to determine whether length or yolk-sac absorption is more important in the establishment of swimming movements.

Some body parts movements were better executed than other in the early developmental stage. The coefficient of variation of r² (CV r²) was found to depend only on the total length of the larvae (Table **2**). CV r² is high (0.5) at the onset of swimming movements but decreased significantly during growth until the fish reached about 11-12 mm TL, after which it stabilized between 0 and 0.05. This stabilization occurred well before the flow regime transition (Fig. **5B**).

The r^2_1 coefficient reached a level of 0.95 when the larvae reached approximately 6.9 mm TL. Beginning at a value close to 0.85, the r^2_2 index was found to increase with increasing length, reaching about 0.95 at 6.2 mm TL. The

Table 3. Results of the Multiple Polynomial Regressions Performed in Order to Characterize the Effects of Size and Relative Swimming Speed on the Variation of the r^2_{mean}, CV r^2, CV $\Delta\varphi$, and *St* indexes in *Clarias gariepinus*.

Determinant	Partial Regression Coefficient	Standard Error of Estimate	0.95 Confidence Interval			Significativity of the Variables (T-test)	
Amplitude LM1 ($F_{4,83}$=82.932, P<0.0001)							
Intercept: 0,5928							
Total length (mm)	-0.1276	0.0126	-0.1523	to	-0.1029	t_{83}=-10.141	P<0.0001
[Total length (mm)]²	0.0093	0.0011	0.0071	to	0.0115	t_{83}=8.2685	P<0.0001
[Total length (mm)]³	-2.00e-04	3.00e-05	-2.59e-04	to	-1.41e-04	t_{83}=-6.9406	P<0.0001
Swimming speed (TL/s)	0.0035	0.0012	0.0011	to	0.0059	t_{83}=2.9547	P=0.0041
Amplitude LM2 ($F_{4,83}$=40.950, P<0.0001)							
Intercept: 0,1331							
Total length (mm)	-0.0254	0.0044	-0.034	to	-0.0168	t_{84}=-5.7401	P<0.0001
[Total length (mm)]²	0.0017	0.0004	0.0009	to	0.0025	t_{84}=4.6887	P<0.0001
[Total length (mm)]³	4.40e-05	1.10e-05	2.24e-05	to	6.56e-05	t_{84}=-4.0096	P=0.0001
Amplitude LM3 ($F_{4,83}$=30.980, P<0.0001)							
Intercept: 0,2061							
Total length (mm)	-0.0398	0.0076	-0.0547	to	-0.0249	t_{83}=-5.2157	P<0.0001
[Total length (mm)]²	0.0028	0.0007	0.0014	to	0.0042	t_{83}=4.1672	P<0.0001
[Total length (mm)]³	0.0036	0.0007	0.0022	to	0.005	t_{83}=-3.4935	P<0.0001
Swimming speed (TL/s)	-6.60e-05	1.90e-05	-1.03e-04	to	-2.88e-05	t_{83}=4.9598	P=0.0007
Amplitude LM4 ($F_{4,83}$=25.481, P<0.0001)							
Intercept: 0,3076							
Total length (mm)	-0.0578	0.0112	-0.0798	to	-0.0358	t_{83}=-5.1642	P<0.0001
[Total length (mm)]²	0.0042	0.001	0.0022	to	0.0062	t_{83}=4.2451	P<0.0001
[Total length (mm)]³	-1.00e-04	2.80e-05	-1.55e-04	to	-4.51e-05	t_{83}=-3.6650	P=0.0004
Swimming speed (TL/s)	0.0038	0.0011	0.0016	to	0.006	t_{83}=3.5613	P=0.0006
Amplitude LM5 ($F_{5,82}$=6.7799, P<0.0001)							
Intercept: 0,2091							
Total length (mm)	-0.0385	0.013	-0.064	to	-0.013	t_{82}=-2.9596	P=0.0040
[Total length (mm)]²	0.0032	0.0012	0.0008	to	0.0056	t_{82}=-2.7330	P=0.0077
[Total length (mm)]³	-8.40e-05	3.20e-05	-1.47e-04	to	-2.13e-05	t_{82}=-2.6048	P=0.0109
Swimming speed (TL/s)	0.01	0.0028	0.0045	to	0.0155	t_{82}=3.6085	P=0.0005
[Swimming speed (TL/s)]³	-7.40e-05	3.10e-05	-1.35e-04	to	-1.32e-05	t_{82}=-2.3847	P=0.0194
Amplitude LM6 ($F_{2,85}$=6.9347, P=0.0016)							
Intercept: 0,0777							
Swimming speed (TL/s)	0.0190	0.0059	0.0306	to	0.0074	t_{85}=3.2051	P=0.0019
[Swimming speed (TL/s)]²	-0.0016	0.0006	-0.0004	to	-0.0028	t_{85}=-2.6247	P=0.0103

Total variance explained for R1, R2, R3, R4, R5 and R6 amplitudes are respectively 80%, 59.4%, 59.9%, 55.1%, 29.3% and 14.0%.

movements of landmarks 3, 4, and 5 were never characterized by r^2 coefficients inferior to 0.95. The r^2_3 and r^2_4 were close to this threshold at the start of our observations. However, they have tendency to increase during growth up to a TL between 7.8 and 8.4 mm. For longer fish, the index values oscillate between 0.98 and 1.00 or 0.99 and 1.00 in the case of r^2_3 and r^2_4, respectively. No tendency could be determined for the r^2_5 coefficient; its values appeared to oscillate randomly between 0.95 and 1.00. In fish exceeding 7.4 mm TL, the r^2_6 index was found to fluctuate in the vicinity of 0.85. So, the middle of the body (r^2_3, r^2_4 and r^2_5) executes adult-like swimming movements from 8 hPH. The anterior part of the body (r^2_1 and r^2_2) will acquire the adult-like movements when the larvae reach 6.9 mm TL. The posterior
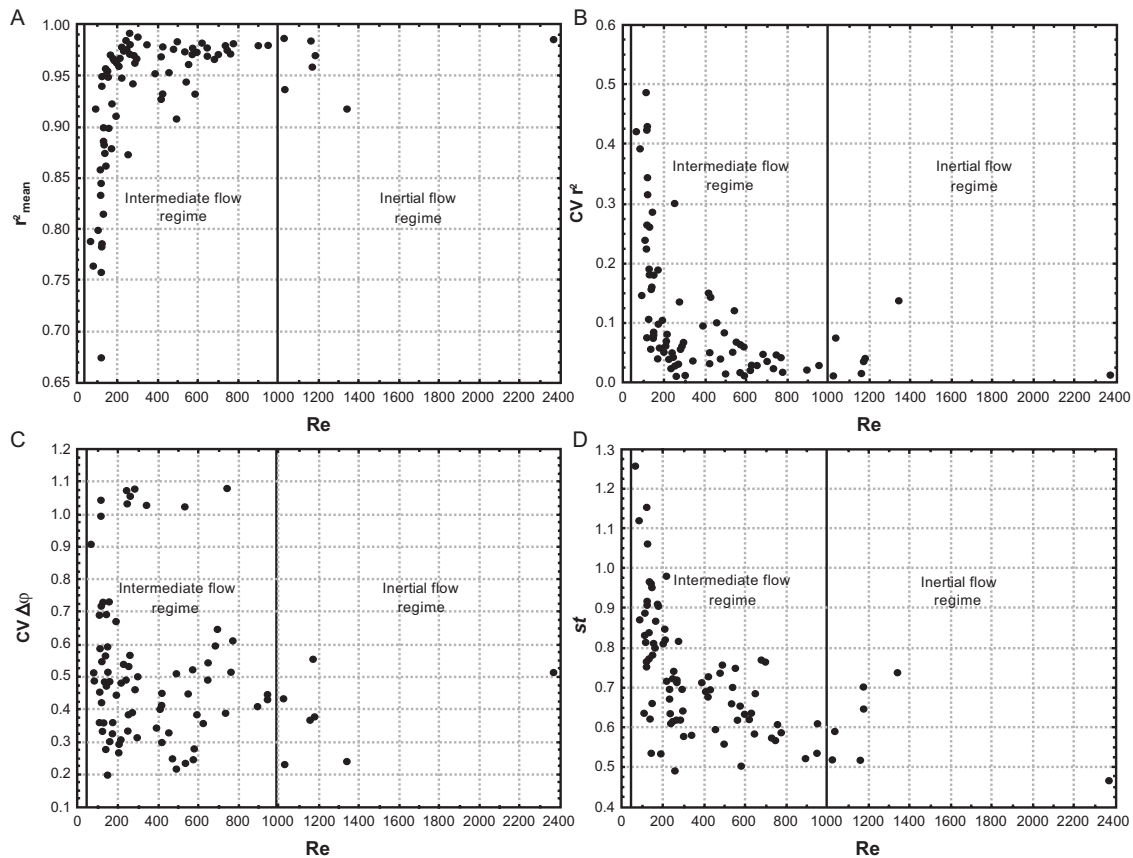
Fig. (5). Plots of r^2_{mean}, CV r^2, CV $\Delta\varphi$, and *St* according to the Reynolds number in *Clarias gariepinus* larvae. The vertical lines indicate a shift in the flow regime. Each circle corresponds to a measurement carried out on one individual.
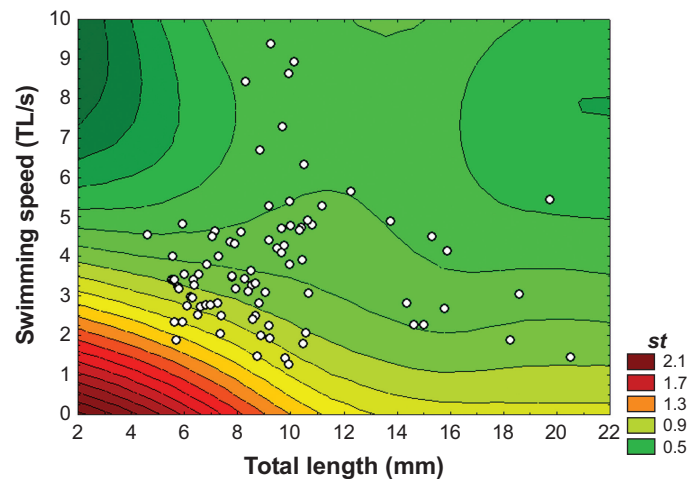

Fig. (6). Variations of the Strouhal number in *Clarias gariepinus* larvae according to the total length and relative swimming speed. The values of the index are given by the color scale. Strouhal number values increase when, while moving on the plot, the color of the area changes from dark green to dark red. White circles: observations made during the present study; each point representing a fish.

part of the body (r^2_6. excluding the tail) will follow pure-sine like trajectory when the larvae reach approximately 7.5 mm TL.

During the whole experiment, they were consistent variations of the propulsive wave speed along the body, independently of the swimming speed. Fluctuations of the coefficient of variation of $\Delta\varphi$ (CV $\Delta\varphi$) were relatively high throughout all the studied part of the ontogeny (from 0.2 to 1.1), although this coefficient tended to decrease as the larvae grew (Table **3**). No relation was found between the relative swimming speed and this coefficient. The hydrodynamic flow regime does not affect the variation of CV $\Delta\varphi$ (Fig. **5C**). CV $\Delta\varphi$ value decrease during growth is correlated with the yolk-sac absorption (R=0.31, P=0.003).

Table 4. Results of the Multiple Polynomial Regressions Performed in Order to Characterize the Effects of Size and Relative Swimming Speed on the Variation of the Amplitude of Each Landmark in *Clarias gariepinus*.

Determinant	Partial Regression Coefficient	Standard Error of Estimate	0.95 Confidence Interval			Significativity of the Variables (T-test)	
Amplitude LM1 ($F_{4,83}=82.932$, $P<0.0001$)							
Intercept: 0,5928							
Total length (mm)	-0.1276	0.0126	-0.1523	to	-0.1029	$t_{83}=-10.141$	P<0.0001
[Total length (mm)]²	0.0093	0.0011	0.0071	to	0.0115	$t_{83}=8.2685$	P<0.0001
[Total length (mm)]³	-2.00e-04	3.00e-05	-2.59e-04	to	-1.41e-04	$t_{83}=-6.9406$	P<0.0001
Swimming speed (TL/s)	0.0035	0.0012	0.0011	to	0.0059	$t_{83}=2.9547$	P=0.0041
Amplitude LM2 ($F_{4,83}=40.950$, $P<0.0001$)							
Intercept: 0,1331							
Total length (mm)	-0.0254	0.0044	-0.034	to	-0.0168	$t_{84}=-5.7401$	P<0.0001
[Total length (mm)]²	0.0017	0.0004	0.0009	to	0.0025	$t_{84}=4.6887$	P<0.0001
[Total length (mm)]³	4.40e-05	1.10e-05	2.24e-05	to	6.56e-05	$t_{84}=-4.0096$	P=0.0001
Amplitude LM3 ($F_{4,83}=30.980$, $P<0.0001$)							
Intercept: 0,2061							
Total length (mm)	-0.0398	0.0076	-0.0547	to	-0.0249	$t_{83}=-5.2157$	P<0.0001
[Total length (mm)]²	0.0028	0.0007	0.0014	to	0.0042	$t_{83}=4.1672$	P<0.0001
[Total length (mm)]³	0.0036	0.0007	0.0022	to	0.005	$t_{83}=-3.4935$	P<0.0001
Swimming speed (TL/s)	-6.60e-05	1.90e-05	-1.03e-04	to	-2.88e-05	$t_{83}=4.9598$	P=0.0007
Amplitude LM4 ($F_{4,83}=25.481$, $P<0.0001$)							
Intercept: 0,3076							
Total length (mm)	-0.0578	0.0112	-0.0798	to	-0.0358	$t_{83}=-5.1642$	P<0.0001
[Total length (mm)]²	0.0042	0.001	0.0022	to	0.0062	$t_{83}=4.2451$	P<0.0001
[Total length (mm)]³	-1.00e-04	2.80e-05	-1.55e-04	to	-4.51e-05	$t_{83}=-3.6650$	P=0.0004
Swimming speed (TL/s)	0.0038	0.0011	0.0016	to	0.006	$t_{83}=3.5613$	P=0.0006
Amplitude LM5 ($F_{5,82}=6.7799$, $P<0.0001$)							
Intercept: 0,2091							
Total length (mm)	-0.0385	0.013	-0.064	to	-0.013	$t_{82}=-2.9596$	P=0.0040
[Total length (mm)]²	0.0032	0.0012	0.0008	to	0.0056	$t_{82}=-2.7330$	P=0.0077
[Total length (mm)]³	-8.40e-05	3.20e-05	-1.47e-04	to	-2.13e-05	$t_{82}=-2.6048$	P=0.0109
Swimming speed (TL/s)	0.01	0.0028	0.0045	to	0.0155	$t_{82}=3.6085$	P=0.0005
[Swimming speed (TL/s)]³	-7.40e-05	3.10e-05	-1.35e-04	to	-1.32e-05	$t_{82}=-2.3847$	P=0.0194
Amplitude LM6 ($F_{2,85}=6.9347$, $P=0.0016$)							
Intercept: 0,0777							
Swimming speed (TL/s)	0.0190	0.0059	0.0306	to	0.0074	$t_{85}=3.2051$	P=0.0019
[Swimming speed (TL/s)]²	-0.0016	0.0006	-0.0004	to	-0.0028	$t_{85}=-2.6247$	P=0.0103

Total variance explained for R1, R2, R3, R4, R5 and R6 amplitudes are respectively 80%, 59.4%, 59.9%, 55.1%, 29.3% and 14.0%.

The swimming efficiency was found to increase during the whole ontogeny and also when the fish swam faster and the yolk-sac disappear. Indeed, the Strouhal number was negatively related to the total fish length (mainly between 4 and 12 mm TL) and swimming speed (Table **3**; Fig. **6**). The variation with swimming speed was greater when the fish were smaller. For a swimming speed of 2 TLs^{-1}, the Strouhal number of a 5.8 mm TL larva was 2.54, as opposed to only 0.98 to 1.92 for fish measuring 10.5 mm TL. For two fish measuring approximately 5.8 mm TL, the value of the Strouhal number was 2.52 at 2 TLs^{-1} and 1.06 at 4.75 TLs^{-1}. A significant correlation was found between the Strouhal number and the volume of the yolk sac (R=0.30, P=0.005). The fish larvae never show Strouhal number in the 0.2 to 0.4

range. Stabilization of this index in the vicinity of 1.2 occurred before the change in the major forces opposing resistance to the swimming fish (Fig. **5D**).

This swimming efficiency increase was followed by a decrease of the lateral displacement of the head (from 13 to 6% of total fish length). This occurred while the total length of the fish increased from 4 to 10 mm TL. Moreover, swimming speed also affected the amplitude of the head since these last increased when the swimming speed increase, independently of the fish total length. These observations were confirmed by multiple polynomial regressions (Table **4**).

Swimming speed of fish could have various consequences on the landmarks located behind the pivot point (Table **4**). First, neither the total fish length nor the relative swimming speed had any influence on the relative amplitude of the landmark located at the tail tip ($F_{2,85}$; P=0.116). Secondly, the movement amplitudes of landmarks 3 to 6 varied as a function of the relative speed of the fish, as shown in the contour plot in Fig. (**7**). For fish having a total length up to

about 10 mm, these amplitudes were found to increase with increasing swimming speed. For longer fish, the amplitudes were still found to increase with speed up to a speed of 5 to 6 TLs^{-1}, but as the speed increased further, the amplitudes decreased (Fig. **7**, LM6, 14 mm TL).

Comparisons between the Adult and the Biggest Larvae

Mann-Whitney U test revealed no differences in landmark trajectories between the five biggest larvae and the adult fish (U=12, P=0.917). No significant difference in CV r² exists between the two groups (U=11, P=0.754). Differences did appear between the adult fish and the five biggest larvae for CV $\Delta\varphi$ (U=0, P=0.009) and the Strouhal number (U=0, P=0.009).

DISCUSSION

Like for other species, *Clarias gariepinus* need to set up their swimming movements since larvae were not able the make displacement at hatching. Swimming movements re-
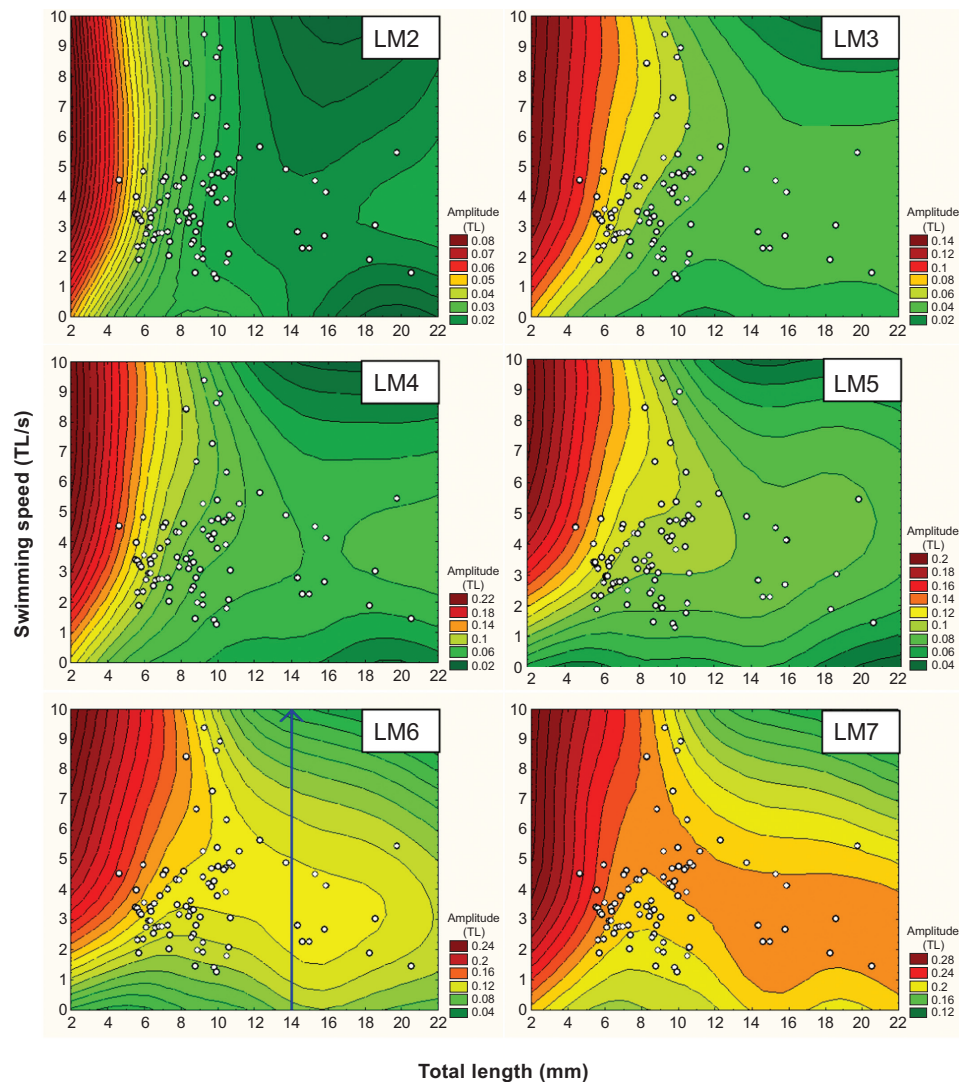

Fig. (7). Surface plot showing the movement amplitudes of landmarks 2 to 7 on *Clarias gariepinus* larvae, in relation to the total fish length and the relative swimming speed of the fish. The amplitude increases when the colored area changes from dark green to dark red. The colored scale is expressed in TL. White circles: observations made during the present study; each spot corresponding to one fish.

sult from the fish muscle activity, the mechanical properties of its skeletal structures, and its interactions with the surrounding medium [35]. Locomotion is an essential function for the survival of organisms because it is involved in numerous behaviors such as avoiding predators, feeding, finding sexual partners, etc. [36]. As most of these behaviors are required early in development, locomotion should appear and be established at an early life stage. Results indicate clearly the total fish length should be used as reference rather than age. In *Clarias gariepinus*, swimming movements were not observed until the larvae reached a total length of 5.3 ± 0.5 mm (approximately 8 hPH). Like the larvae of *Cyprinus carpio* [37] and *Danio rerio* [5], *C. gariepinus* larvae swim first by producing non-sinusoidal movements. The ontogeny of adult-like swimming movements does not appear simultaneously all along the body of the fish. The central part of the body is the first to show lateral displacements very close to the theoretical sinusoids observed in adults. From this region, improvement progresses simultaneously in the directions of the head and tail, but the anterior part of the body achieves completely adult-like movements well before the rear part. Once initiated, the development of swimming movements is quickly achieved, reaching the adult level of organization at 7 to 8 mm TL (in function of the swimming speed; about 48 hPH), stage at which the yolk-sac volume is almost fully resorbed. In larvae, the movements of the caudal extremity of the body rarely approach the theoretical sinusoids. The caudal fin might follow more or less passively the movements of the rest of the body.

The rapid development of anguilliform swimming movements could be in relation with the main environmental constraints acting on small sized fishes: the viscosity of the medium [38]. During the absorption of the yolk sac, the surface area opposed to the medium decrease. This allows the fish to better penetrate in the water and to decrease the importance of the viscous force. A swimming mode using undulations, and more precisely the anguilliform swimming mode, is adapted to all types of hydrodynamic flow regime and more specially to the viscous one and is thus practiced in a first time by the larvae like *C. gariepinus* [15, 39, 40]. This assumption is reinforced by previous studies: fishes having subcarangiform mode of swimming at adult stage (*Danio rerio*, *Cyprinus carpio*) present first anguilliform swimming mode during their larval stage until they reach the inertial flow regime [6, 10].

The development of anguilliform movements is not only due to the acquisition of the wave along the body. Other factors allow to increase the swimming efficiency. At hatching, larvae execute swimming movements of great amplitude all along the body. During growth, all the landmarks were found to move with lesser amplitude. This amplitude reduction affected the head-tip landmark most markedly. A reduced amplitude of the anterior part of the body enables a fish to increase its swimming efficiency by decreasing the drag and the energy cost involved in displacement. However, increased head-movement amplitudes in *C. gariepinus* larvae corresponded to increasing swimming speed, as for the adult eel *Anguilla rostrata* (Lesueur) [33]. It results from a larger recruitment of the muscles of the anterior region required to increase the speed [41, 42]. On the other hand, the relative

amplitude of the tail does not vary significantly in relation to the swimming speed in *C. gariepinus*. Batty [12], Videler and Wardle [38] and Tytell [43] working respectively on *Pleuronectes platessa* larvae and on adult individuals of various species (*i.e. Gadus morua* L., *Anguilla rostrata*), reached to the same conclusion.

The amplitude of the landmark placed on the fish head was not the only one affected by the swimming speed. From 10 mm TL, the movement amplitudes of landmarks 3 to 6 in *C. gariepinus* increase when fish accelerate up to a speed included between 5 and 6 TLs^{-1}. Thereafter (>6TLs^{-1}), the amplitude of LM 3 to 6 tended to decrease. This suggests that at very high speed, a fish might be able to increase the rigidity of part of its body. This supports the hypothesis of McHenry *et al.* [44], who propose that by increasing body rigidity, adult fish can control their swimming speed by maintaining constant the wavelength of the wave of curvature. Body control can be achieved by antagonistic actions of certain muscles [2, 22, 45, 46]. Increased body rigidity might also allow better penetration of the water mass, further increasing the flow of fluid around the body of the larva.

The swimming efficiency appeared to be dependant of the swimming speed for *Clarias gariepinus*. This is in accordance with results obtained for some species, but not for all. The relationship between Strouhal number and efficiency is well known and used for adult fish, i.e. at high Reynolds numbers [32, 33]. *Clarias gariepinus* adults do not practice an efficient swimming mode when swimming between 1 and 2 TLs^{-1}. However, the movement is fully efficient for the fish swimming at 4.5 TLs^{-1}. Consequently, Strouhal values change with the swimming speed. This situation is different from the one observed for the adult eels (*Anguilla rostrata*) since Tytell [43] observed no variation of the Strouhal number with swimming speed. However, some species are known to have an efficiency dependent of the swimming speed like *C. gariepinus* such as the salmoniform *Oncorhynchus tshawytscha* (Walbaum) [33]. The latter species, however, does not practice an anguilliform swimming mode but a subcarangiform one.

We report our results treating of the variations of the Strouhal number in *C. gariepinus* larvae even though we cannot interpret them in terms of efficiency, as the relationship between the Strouhal number and efficiency is poorly known at low Reynolds number (<1000). Our aim was to describe the way in which the values of the index change during growth until they reach the values observed for the adults. A great variation of Strouhal values (from 2.4 to 1.2) was observed in the first developmental stages (8 and 12hPH). At 12 mm TL, when the head movements had diminished and the yolk sac is absorbed, the maximal value observed was 1.4. These two events could play significant roles in the increase of the relative swimming efficiency of the fish larvae. As in the case of adult *C. gariepinus*, the Strouhal number values recorded for fish measuring more than 12 mm TL tended to decrease significantly with increasing swimming speed. Yet before the theoretical change in flow regime, the Strouhal number was found to stabilize in larvae at a value around 1.2. Since adults display lower values of this index (*St*<0.8), we deduce that it must decrease further between the stage corresponding to the biggest larvae

studied and the adult stage, well after the transition of flow regime.

Another challenge in swimming ontogeny is found in the shift of hydrodynamic regime. Larvae possess a small Re and swims in an intermediate flow regime whereas adults having a high Re move in an inertial flow regime [6]. In *C. gariepinus*, some adult-like movement, such as the motion of each landmark, and the swimming-movement efficiency, were adopted before the theoretical change in hydrodynamic flow regime. All notable modifications of the various studied parameters occur before the change in hydrodynamic flow regime, which thus does not seem to affect how swimming movements are executed. Complementary measurements should be performed, however, to acquire more information on what happens to fish swimming in an inertial flow regime.

CONCLUSION

In conclusion, swimming movements are not established in *C. gariepinus* larvae until 48 hours post-hatching (between 7 and 8 mm TL), stage at which the yolk-sac volume is fully resorbed. Both adults and larvae with established swimming movements practice an anguilliform swimming mode. In parallel with growth and the disappearance of the yolk sac, the establishment of swimming movements is accompanied by a strong reduction in lateral movement of the head. However, these head movements are correlated with swimming speed, tending to increase as a fish accelerates. In contrast, the relative lateral amplitude of tail movements does not appear to correlate with either the total fish length or the relative swimming speed. Interestingly, none of the monitored indexes shows any major change at the transition from the intermediary to the inertial flow regime. Some data suggest that larvae can increase their body rigidity with increasing swimming speed.

ACKNOWLEDGEMENTS

REFERENCES

[1]   Gray J. Studies in animal locomotion: I. The movement of fish with special refrence to the eel. J Exp Biol 1933; 10: 88-104.

[2]   Blight AR. The muscular control of vertebrate swimming movements. Biol Rev 1977; 52: 181-218.

[3]   Videler JJ. Fish swimming. London: Chapman & Hall, 1993.

[4]   Wardle CS, Videler JJ, Altringham JD. Tuning in to fish swimming waves: body form, swimming mode and muscle function. J Exp Biol 1995; 198: 1629-36.

[5]   Müller UK, Van Leeuwen JL. Swimming of larval zebrafish: ontogeny of body waves and implications for locomotory development. J Exp Biol 2004; 207: 853-68.

[6]   Fuiman LA, Webb PW. Ontogeny of routine swimming activity and performance in *Zebra danio* (Teleostei; Cyprinidae). Anim Behav 1988; 36: 250-61.

[7]   Müller UK, van den Boogaart JGM, van Leeuwen JL. Flow patterns of larval fish: undulatory swimming in the intermediate flow regime. J Exp Biol 2008; 211: 196-205.

[8]   Fontaine E, Lentink D, Kranenbarg S, *et al.* Automated visual tracking for studying the ontogeny of zebrafish swimming. J Exp Biol 2008; 211 (8): 1305-16.

[9]   Osse JWM. Form changes in fish larvae in relation to changing demands of function. Neth J Zool 1990; 40: 362–85.

[10]   Osse JWM, Van den Boogaart JGM. Body size and swimming types in carp larvae: effects of being small. Neth J Zool 2000; 50 (2): 233-44.

[11]   Osse JWM, Van de Boogaart JGM. Dynamic morphology of fish larvae, structural implications of friction forces in swimming, feeding and ventilation. J Fish Biol 1999; 55 (suppl. A): 156-74.

[12]   Batty RS. Locomotion of plaice larvae. Symp Zool Soc Lond 1981; 48: 53-69.

[13]   Batty RS. Observation of fish larvae in the dark with television and infra-red illumination. Mar Biol 1983; 76: 105-7.

[14]   Batty RS. Development of swimming movements and musculature of larval herring (*Clupea harengus*). J Exp Biol 1984; 110: 217-29.

[15]   Webb PW, Weihs D. Functional locomotor morphology of early life history stages of fishes. Trans Am Fish Soc 1986; 115: 115-27.

[16]   McHenry MJ, Azizi E, Strother JA. The hydrodynamics of locomotion at intermediate Reynolds numbers: undulatory swimming in ascidian larvae (Botrylloides sp.). J Exp Biol 2003; 206 (2): 327-43.

[17]   Sfakiotakis M, Lane DM, Davies JBC. Review of fish swimming modes for aquatic locomotion. IEEE J Ocean Eng 1999; 24 (2): 237-52.

[18]   Fuiman LA, Batty RS. What a drag it is getting cold: partitioning the physical and physiological effects of temperature on fish swimming. J Exp Biol 1997; 200: 1745–55.

[19]   McHenry MJ, Lauder GV. The mechanical scaling of coasting in zebrafish (*Danio rerio*). J Exp Biol 2005; 208: 2289-301.

[20]   Halle ME. Locomotor mechanics during early life history: effects of size and ontogeny on fast-start performance of salmonid fishes. J Exp Biol 1999; 202: 1465-79.

[21]   Carrier DR. Ontogenetic limits on locomotor performance. Physiol Zool 1996; 69: 467-88.

[22]   Long JH, McHenry MJ, Boetticher NC. Undulatory swimming: How traveling waves are produced and modulated in sunfish (*Lepomis gibbosus*). J Exp Biol 1994; 192: 129-45.

[23]   Long JH, Nipper KS. The importance of body stiffness in undulatory propulsion. Am Zool 1996; 36: 678-94.

[24]   Osse JWM, Van den Boogaart JGM. Fish larvae, development, allometric growth, and the aquatic environment. ICES Mar Sci Symp 1995; 201: 21-34.

[25]   Weihs D. The mechanism of rapid starting in slender fish. Biorheology 1973; 10: 343-50.

[26]   Van Raamsdonk W, Pool C, Kronnie G. Differentiation of muscle fiber types in the teleost *Brachydanio rerio*. Anat Embryol 1978; 153: 137-55.

[27]   Videler JJ. Swimming movements, body structure and propulsion n cod *Gadus morhua*. Symp Zool Soc Lond 1981; 48: 1-27.

[28]   Kamler E, Szlaminska M, Kuczynski M, Hamackova J, Kouril J, Dabrowski R. Temperature-induced changes of early development and yolk utilization in the african catfish *Clarias gariepinus*. J Fish Biol 1994; 44: 311-26.

[29]   Almazan-Rueda P, Helmond ATMV, Verreth JAJ, Schrama JW. Photoperiod affects growth, behaviour and stress variables in *Clarias gariepinus*. J Fish Biol 2005; 67: 1029-39.

[30]   Triantafyllou GS, Triantafyllou MS, Grosenbaugh MA. Optimal hrust development in oscillating foils with application to the fish propulsion. J Fluids Struct 1993; 7: 205-24.

[31]   Triantafyllou MS, Triantafyllou GS, Gopalkrishnan R. Wake mechanics of thrust generation in oscillating foils. Phys Fluids 1991; 3(12): 2835-7.

[32]   Taylor GK, Nudds RL, Thomas ALR. Flying and swimming animals cruise at a Strouhal number tuned for high power efficiency. Nature 2003; 425: 707-10.

[33]   Lauder GV, Tytell ED. Hydrodynamics of undulatory propulsion. In: Shadwick RE, Lauder GV, Eds. Fish Biomechanics. Academic Press. New-York: Elsevier; 2006; p. 542.

[34]   Lighthill J. Mathematical biofluiddynamics. mathematics Sfiaa, editor. Philadelphia SIAM; 1975.

[35]   Videler JJ. Fish swimming movements: a study of one element of behaviour. Neth J Zool 1985; 35 (1-2): 170-85.

[36]   Houde. Patterns and consequences of selective processes in teleost early life histories. In: Chambers RC, Trippel EA, Eds. Early life history and recruitment in fish populations. London: Chapman & Hall; 1997. p. 173-96.

[37]   Osse JWM, Van den Boogaart JGM. Dynamic morphology of fish arvae, structural implications of friction forces in swimming, eeding and ventilation. J Fish Biol 1999; 55 (Suppl. A): 156-74.

[38]   Videler JJ, Wardle CS. Fish swimming stride by stride: speed limits and endurance. Rev Fish Biol Fish 1991; 1: 23-40.

[39]   Grey J, Hancock GJ. The propulsion of sea-urchin spermatozoa. J Exp Biol 1955; 32: 775-801.

[40]   Lighthill MJ. Hydrodynamics of aquatics animal propulsion - a survey. Annu Rev Fluid Mech 1969; 1: 413-46.

[41]   Webb PW. 'Steady' swimming kinematics of tiger musky, an esociform accelerator, and rainbow trout, a generalist cruiser. J Exp Biol 1988; 138: 51-69.

[42]   Lighthill MJ. Aquatic animal propulsion of high hydromechanical efficiency. J Fluid 1970; 44: 265-301.

[43]   Tytell ED. The hydrodynamics of eel swimming: II. Effect of swimming speed. J Exp Biol 2004; 207: 3265-79.

[44]   McHenry MJ, Pell CA, Long JH. Mechanical control of swimming speed: stiffness and axial wave form in undulating fish models. J Exp Biol 1995; 198: 2293–305.

[45]   Van Leeuwen JL, Lankeet MJM, Akster HA, Osse JWM. Function of red muscles of carp (*Cyprinus carpio*): recruitment and normalized power output during swimming in different modes. J Zool 1990; 220: 123-45.

[46]   Altringham JD, Wardle CS, Smith CI. Myotomal muscle function at different locations in the body of a swimming fish. J Exp Biol 1993; 182: 191-206.